Infrared Physics and Technology 105 (2020) 103219

Contents lists available at ScienceDirect

Infrared Physics & Technology

journal homepage: www.elsevier.com/locate/infrared

Computer aided detection of diabetic foot ulcer using asymmetry analysis of texture and temperature features

J. Saminathan[a,*], M. Sasikala[a], VB. Narayanamurthy[b], K. Rajesh[b], R. Arvind[b]

[a] Department of Electronics and Communication Engineering, CEG Campus, Anna University, Chennai, Tamil Nadu, India
[b] Hycare for Wounds, Chennai, Tamil Nadu, India

ARTICLE INFO

Keywords:
Diabetic foot
Asymmetry analysis
Foot ulcer
Thermal Image
Temperature
Texture
Support vector machine

ABSTRACT

Diabetic foot ulcer is a foremost complication of poorly controlled diabetes mellitus leading to lower extremity amputation. Early identification depends on repeated risk assessment, preferably on a day-to-day basis especially for high-risk patients. The temperature variations in the areas prone to ulcer are higher than non-ulcerous regions of the foot. The ultimate aim of this study was to develop an efficient algorithm for early detection of diabetic foot with infrared thermal images using asymmetry analysis. The left and right foot regions are segmented using region growing method. In normal plantar thermograms, symmetric temperature distributions are observed, whereas, in the case of the diabetic foot, asymmetry was observed between ipsilateral and contralateral regions of the foot. The texture and temperature features are extracted from the 11 regions of interest from the foot and asymmetric analysis was performed for the features extracted from the ipsilateral and contralateral regions of the foot. Support vector machine was used to classify the region of interest into normal and ulcer. The proposed method achieved maximum accuracy of 95.61%, sensitivity of 96.5% and specificity of 92.41%. The performance of the proposed technique shows that it is trustworthy and effective for early identification of pre-signs of ulceration and aids the clinicians in the treatment of the diabetic foot.

1. Introduction

Diabetes is a chronic disease characterized by hyperglycemia resulting from defects in insulin secretion, insulin action, or both. The chronic hyperglycemia of diabetes is associated with long-term damage, dysfunction, and failure of different organs, especially the eyes, kidneys, nerves, heart, and blood vessels [1]. The International Diabetes Federation (IDF) reports that currently there are 382 million people with diabetes worldwide and by 2035 this number is expected to increase up to 592 million people [2,3]. People with chronic diabetes and people with poor circulation are prone to diabetic foot ulcer that occurs due to the destruction of deep tissue in the lower limb. Foot ulcers are especially common in people who have one or more of the health complications such as peripheral neuropathy, circulatory problems, and abnormalities in the bones or muscles of the feet [4]. A vascular and neurological disorder in lower extremities is one of the common complications with Diabetes Mellitus (DM). Critical foot complications arise at the future stage of DM and are in about 15%–25% of diabetic patients and among them, 6% of the people will be hospitalized. These foot problems arise as a consequence of foot ulceration, infection and also due to peripheral ischemia. Peripheral neuropathy and lower extremity ischemia due to peripheral artery disease are the principal causes of diabetic foot ulcers, which affects the capability of the foot to feel and sense. Common signs and symptoms of a diabetic foot ulcer include numbness, the appearance of drainage on the person's socks, redness, unusual swelling, and regions with increased temperature [5,6].

Infrared (IR) thermal imaging cameras have been increasingly used in clinical situations for accurate and objective thermal mapping of the human body, particularly as a complementary, noninvasive, non-radioactive diagnostic method [5,7–12,35,36,38]. A blackbody or a full radiator is defined as a radiator of uniform surface temperature whose radiant exitance in all parts of the spectrum is the maximum obtainable. The emissivity of a full radiator is unity for all wavelengths. Since the human skin has an emissivity value of 0.98, thus making it more competent for the measurement of temperature distribution using infrared thermal imaging system [9]. The thermal image of the foot gives a complete representation of the distribution of temperatures in the plantar region [10]. Several studies report that the ulceration caused by inflammation that has occurred at the site of measurement is indicated in terms of temperature increase greater than 2.2 °C between right and left foot. [3,13–17,35]. Comparison of temperature distributions of both the feet from the same subject is made and this information is

* Corresponding author.
E-mail address: saminathan23@yahoo.in (J. Saminathan).

https://doi.org/10.1016/j.infrared.2020.103219
Received 3 August 2019; Received in revised form 24 January 2020; Accepted 26 January 2020
Available online 29 January 2020

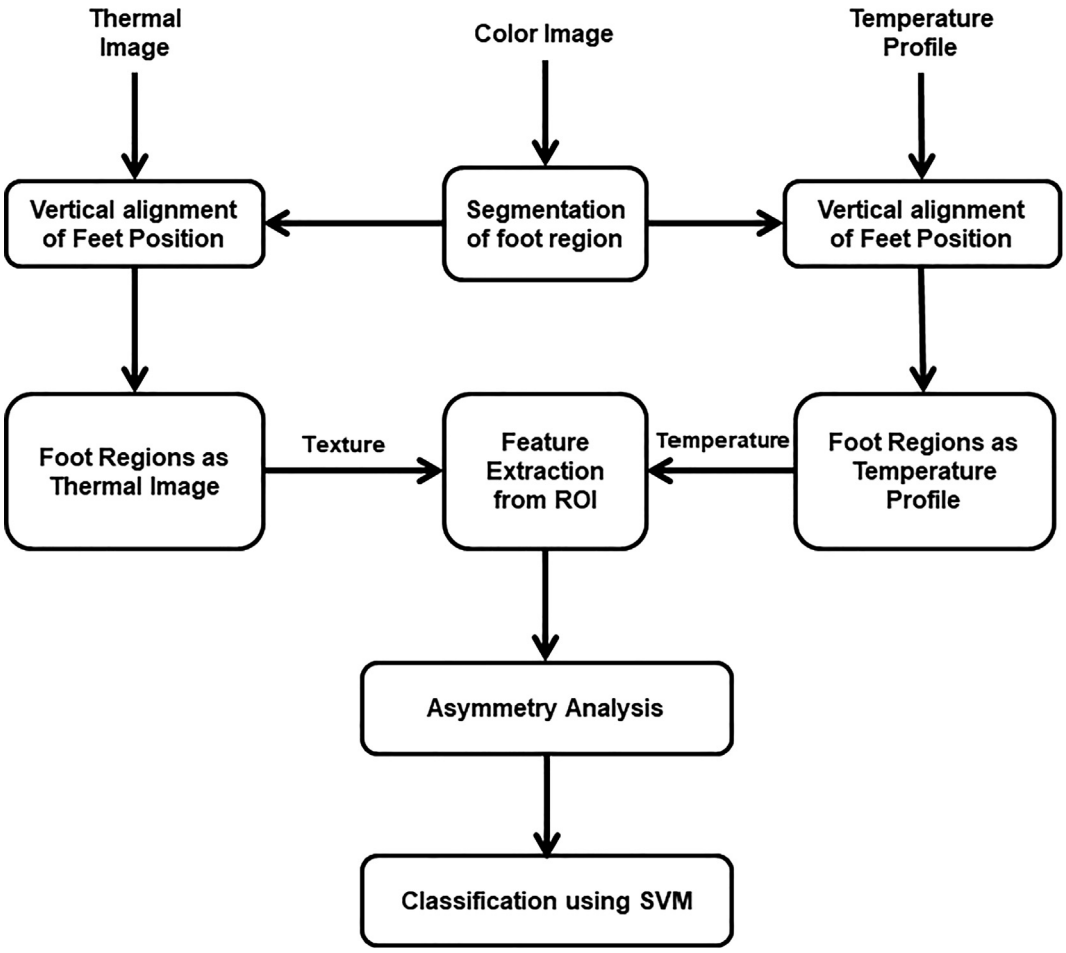

Fig. 1. Schematic flowchart of the proposed methodology.

combined to predict the ulcers using a thresholding technique [18]. The texture and temperature distributions are different for control and for patients who have diabetic foot complications. Symmetric texture and temperature distributions are observed in foot thermogram of control foot whereas asymmetry is observed when there is foot complication in one of the foot regions. From the literature, it is inferred that asymmetric analysis in temperature distribution and external stress analysis have been the most common analyses for identifying diabetic foot complications, while the distribution of texture analysis has been least used so far.

The main objective of this study is to develop an efficient algorithm for early detection of diabetic foot with infrared thermal images using asymmetry analysis of both texture and temperature features. Texture and temperature features are extracted from the plantar foot thermal images. A support vector machine (SVM) is trained to classify the features into normal or prone to an ulcer.

2. Materials and methods

The proposed schematic flow for early detection of diabetic foot ulcer is shown in Fig. 1. The thermal image and color image of the foot are acquired using the FLIR E60 thermal imaging camera. The left and right foot regions are segmented from the color image of the foot using region growing algorithm. These foot regions are used to segment the foot regions from the thermal image and temperature profile of the foot. Textural and temperature features are extracted and asymmetric analysis is performed for most prone areas which can develop diabetic foot ulcer. These features are used to train the support vector machine and classify the region of interest as normal or prone to an ulcer.

2.1. Thermal imaging camera

Most of the work in the plantar foot thermography has been done on thermograms acquired using infrared thermal imaging camera. Thermal imaging cameras with a finer resolution made for medical applications are able to measure subtle changes in temperature and hence are capable of improved detection of diabetic foot complications. A FLIR E60 thermal imaging camera is used for the present study to acquire plantar foot thermal images. It has a resolution of 320 × 240 pixels and covers a field of view (FOV) of 25° × 19°. The range of operation of the camera is in the region of the infrared spectrum from 7.5 μm to 13 μm wavelength. It has the ability to detect the temperature in the range of −20°C to 650°C with thermal sensitivity of less than 0.07 °C at 30 °C and has an onboard digital camera with a resolution of 3.1 megapixels (MP). The onboard digital camera covers the same FOV as that of thermal imaging camera and acquired images are of size 2048 × 1536 pixels. The temperature values are associated with a color palette (Rainbow Color Scheme palette) in order to represent and distinguish them graphically. It is ensured that the thermal imaging camera is calibrated against a black body reference as per the manufacturer's recommendations [20].

2.2. Image acquisition protocol

Thermal image and color image of the plantar foot are acquired from sixty subjects in the present work, out of which 24 are non-diabetic subjects that form the control group and 36 with diagnosed diabetes that forms the DM group. Both control and DM groups include male and female participants, aged between 30 and 65 years. Ethical

Fig. 2a. Color image of the foot – control.

approval was sought and granted by the Institution Ethics Committee of Hycare for Wounds, Chennai. All the participants provided their written informed consent to take part in this study. The experimental room is shielded from any other available infrared (IR) radiation source. Thermal imaging camera is positioned perpendicular to the plane of acquisition at a distance of 1.1 m. The thermal images are obtained in a closed room with a controlled temperature of 20 ± 2℃. During the examination, the participants are seated fairly equidistant and adequately spaced from each wall. The subjects are instructed to remove the footwear to clean their foot by wiping them thoroughly using a damp towel. Subsequently, the participants remained barefooted for 10–15 min before the acquisition of thermal images to achieve equilibrium with the contrast ambient temperature [5,6,9,10,21–24,32–34,37].

A uniform backdrop is placed to ensure a homogenous background. The regions prone to ulcer, determined by wound care specialists, was considered as ulcer regions for the classification of the region of interests. The acquired images of the plantar foot of a participant from the control group and DM group with the onboard digital camera and thermal imaging camera, are shown in Figs. 2(a), 2(b) and Figs. 3(a), 3(b) respectively. The temperature profile (320 × 240) for all the pixel of the acquired thermal image, are exported to comma-separated values (CSV) format with the help of FLIR research and development software.

2.3. Segmentation of foot region

Color images (images acquired through the onboard digital camera) of the plantar foot are converted to grayscale and divided into two sub-images of size 240 × 160, in which first sub-image represents the left

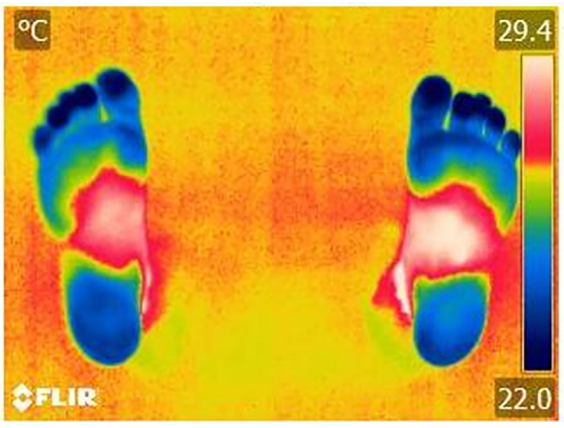

Fig. 2b. Thermal image of the foot – control.

Fig. 3a. Color image of the foot – diabetes mellitus.

Fig. 3b. Thermal image of the foot – diabetes mellitus.

foot and second sub-image represents the right foot. The left and right foot regions are segmented without background using region growing algorithm [25]. The initial seed pixel was fixed at the midpoint of the foot region. The region is grown from the initialized seed pixel by adding in adjacent pixels that are similar, increasing the size of the region. An initial set of small areas are iteratively appended according to the similarity constraints until there are no modifications in two successive iterative stages. The segmented foot regions are in the form of a binary image (foreground or foot region as 1 and background as 0).

2.4. Vertical alignment of feet position

A participant's left foot and right foot does not persist vertical position in resting position during the image acquisition of plantar foot. Instead, they are laterally displaced. The feet position is corrected by drawing a segment from the centroid of the foot to the center of the calcaneal base (the heel). The orientation angle is calculated between the center of the calcaneal base with respect to a perpendicular line from the centroid of the segmented foot region. Then the right and left foot regions are rotated around the centroid for the orientation angle to make the vertical alignment of the foot region, which is depicted in Figs. 4a and 4b. The thermal image of the foot region and temperature profile are also rotated in the same manner for both the left and right foot. The binary image of the segmented foot regions is multiplied with the red, green and blue planes of the respective foot image and concatenated together to get the segmented foot regions from the thermal image. The segmented left and right foot regions of the control group and DM group are illustrated in Figs. 5a and 5b, respectively. The binary image of the segmented foot regions is multiplied with the

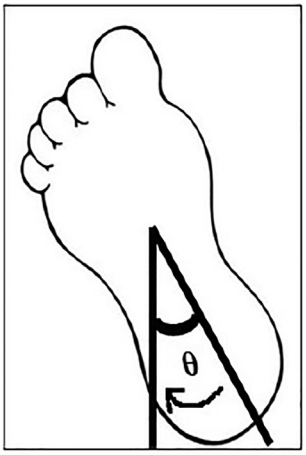

Fig. 4a. Vertical alignment of right foot.

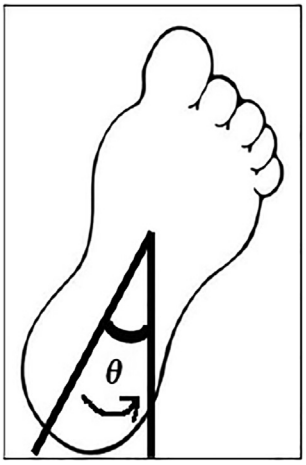

Fig. 4b. Vertical alignment of left foot.

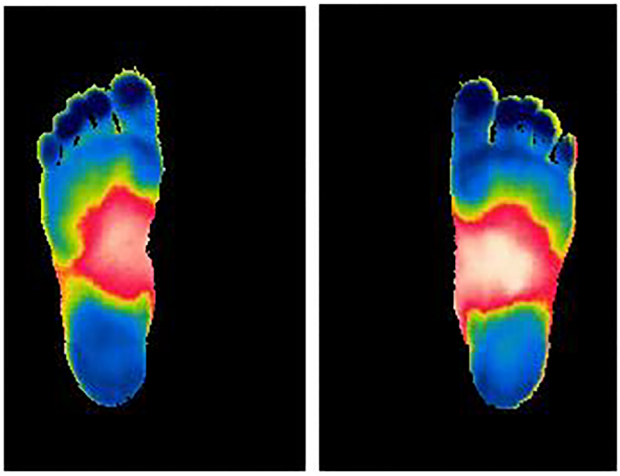

Fig. 5a. Segmented left and right foot regions of the Control Group.

temperature profile of the corresponding foot regions to acquire the temperature distribution for foot regions.

2.5. Feature extraction

The toe apices (great toe, index toe, middle toe, fourth toe, little toe), 5 metatarsal heads behind the phalanges of the toe apices and

Fig. 5b. Segmented left and right foot regions of the DM Group.

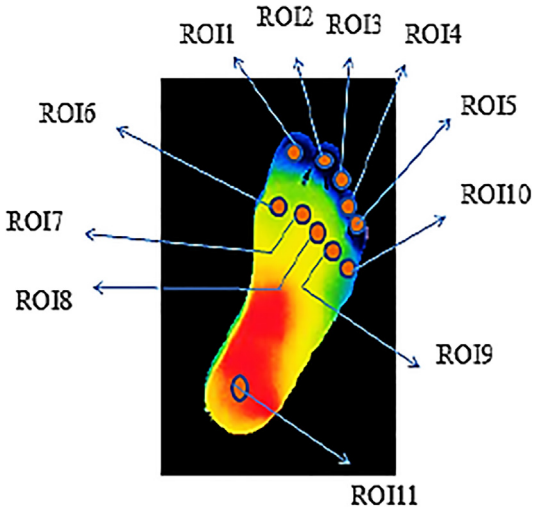

Fig. 6. Primary regions 'at risk' for developing diabetic foot complications.

calcaneal heel are considered as primary regions of interest (ROI) 'at risk' for developing diabetic foot ulcer [26,27]. These regions are selected in both the foot regions as shown in Fig. 6. These eleven ROIs (ROI1 – ROI11) are selected from segmented left and right foot regions manually and converted to grayscale. Similarly, the same eleven ROIs are selected from the temperature distribution of both the foot regions. The mean and standard deviation (SD) of temperature is found for all ROIs and stored as feature vectors for further processing. The following equations define these features

(1) Mean temperature

$$f_1 = \frac{1}{N}\sum_{i=1}^{N} T_i \tag{1}$$

(2) Standard deviation of temperature

$$f_2 = \sqrt{\frac{1}{N-1}\sum_{i=1}^{N} |T_i - f_1|^2} \tag{2}$$

The gray level co-occurrence matrix (GLCM), a renowned statistical technique based on joint probability distribution of pair of pixels is used for extracting second order texture features from ROIs in this study.

An image with the size of $M \times N$ pixels and L gray levels could illustrate the frequency of pixel (i.e.) at the position $[x + d_x, y + d_y]$ that occur with gray level j and in accordance with a distance d from a certain pixel at the position (x, y) with gray level i. The frequency is

denoted by P and its mathematical expression is given as

$$p_{(i,j,d,\theta)} = \sum_{x=1}^{K}\sum_{y=1}^{K}\begin{Bmatrix} 1, & if\ I(x,y)=i \text{ and } I(x+d_x, y+d_y)=j \\ 0, & Otherwise \end{Bmatrix} \quad (3)$$

where (x, y) denotes the coordinates of the image I, pixel i and j are the gray values. d_x and d_y denote the position offsets d is the step, θ is the direction. Once the GLCM in a certain direction is constructed, $p_{(i,j,d,\theta)}$ needs to be normalized to ensure that its feature is not influenced by the regions limitations. The normalized $p_{(i,j,d,\theta)}$is

$$p_{(i,j,d,\theta)} = \frac{p_{(i,j,d,\theta)}}{R} \quad (4)$$

If $\theta = 0^{\circ}$, R is taken as$2M \times (N-1)$
If $\theta = 90^{\circ}$, R is taken as$2N \times (M-1)$
If $\theta = 45^{\circ} = 135^{\circ}$, R is taken as $2(M-1) \times (N-1)$.

For a given offset distance, co-occurrence matrices are calculated for offset angle of 0° and 12 GLCM texture features are derived in this study. The features are defined in equation numbers 9–20. Let $p(i, j)$ be the (i, j)th entry in the normalized GLCM [28–31]. The mean and standard deviation for rows and columns of the matrix are

$$\mu_x = \sum_i \sum_j i \cdot p(i,j) \quad (5)$$

$$\mu_y = \sum_i \sum_j j \cdot p(i,j) \quad (6)$$

$$\sigma_x = \sum_i \sum_j (i-\mu_x)^2 \cdot p(i,j) \quad (7)$$

$$\sigma_y = \sum_i \sum_j (j-\mu_y)^2 \cdot p(i,j) \quad (8)$$

The texture features are as follows.

(3) Autocorrelation

$$f_3 = \sum_i \sum_j (ij) p(i,j) \quad (9)$$

(4) Contrast

$$f_4 = \sum_{n=0}^{N_g-1} n^2 \left\{ \sum_{i=1}^{N_g}\sum_{j=1}^{N_g} p(i,j) \,||i-j| = n \right\} \quad (10)$$

(5) Correlation

$$f_5 = \frac{\sum_i \sum_j (ij) p(i,j) - \mu_x \mu_y}{\sigma_x \sigma_y} \quad (11)$$

(6) Dissimilarity

$$f_6 = \sum_i \sum_j |i-j|\ p(i,j) \quad (12)$$

(7) Energy

$$f_7 = \sum_i \sum_j p(i,j)^2 \quad (13)$$

(8) Entropy

$$f_8 = -\sum_i \sum_j p(i,j) \log(p(i,j)) \quad (14)$$

(9) Homogeneity

$$f_9 = \sum_i \sum_j \frac{1}{1+(i-j)^2} p(i,j) \quad (15)$$

(10) Maximum Probability

$$f_{10} = \underset{(i,j)}{MAX} p(i,j) \quad (16)$$

(11) Sum of Squares: Variance

$$f_{11} = \sum_i \sum_j (i-\mu)^2 p(i,j) \quad (17)$$

(12) Sum Average

$$f_{12} = \sum_{i=2}^{2N_g} i p_{x+y}(i) \quad (18)$$

(13) Sum Entropy

$$f_{13} = -\sum_{i=2}^{2N_g} p_{x+y}(i) \log(p_{x+y}(i)) \quad (19)$$

(14) Sum Variance

$$f_{14} = \sum_{i=2}^{2N_g} (i-f_{11})^2 p_{x+y}(i) \quad (20)$$

The above twelve texture features are extracted from the GLCM of the all eleven ROIs for both left and right foot region and stored as feature vectors in the database for training the network.

2.6. Asymmetry analysis

Asymmetry analysis is an indicator used to determine the difference in the extracted texture and temperature features between ipsilateral and contralateral foot regions (ROIs) [18,19,33,34]. The GLCM texture features and temperature features are extracted from all the 11 ROIs in left and right foot regions. The ROI-1 of temperature features and texture features of right foot region is subtracted from the ROI-1 of temperature features and texture features of left foot region to get the asymmetric analysis between the left foot and right foot. This process is performed in the similar method for the remaining ROIs (ROI-2 to ROI-11). In the foot thermograms of the control group, symmetric temperature distributions are habitually observed in both foot region and, hence, texture and temperature features extracted from ipsilateral and contralateral regions of the foot (ROIs) are almost the same. Thus, the difference in feature values between them will be negligible. However, this difference will be noteworthy in the case of diabetic foot complications, due to the inherent thermal asymmetry between the ipsilateral and contralateral region of foot regions.

2.7. Classification using SVM

Support Vector Machine (SVM) is a discriminative classifier algorithm, in regard to the patterns represented by the subset $d_i = +1$ and the patterns represented by the subset $d_i = -1$ are linearly separable. The decision surface that is in the form of a hyperplane that does the separation is given as follows.

$$w^T x = \sum_i w_i x_i \quad (21)$$

$$w^T x + b = 0 \quad (22)$$

where x is an input vector, w is an adjustable weight vector and b is bias. The point closest to hyperplane is called the 'support vector'. The SVM classifier maximizes the margin of separation (ρ) between the classes and minimizes the classification errors [32]. SVM classifies the input feature vectors by finding the best hyperplane that separates all data points of one class (control group) from those of the other class (DM group). The best hyperplane for SVM is the one with the largest margin between the two classes as illustrated in Fig. 7. The classification performance of SVM classifier is evaluated by the following metrics.

$$Accuracy = \frac{TP+TN}{TP+TN+FP+FN} \times 100\% \quad (23)$$

$$Sensitivity = \frac{TP}{TP+FN} \times 100\% \quad (24)$$

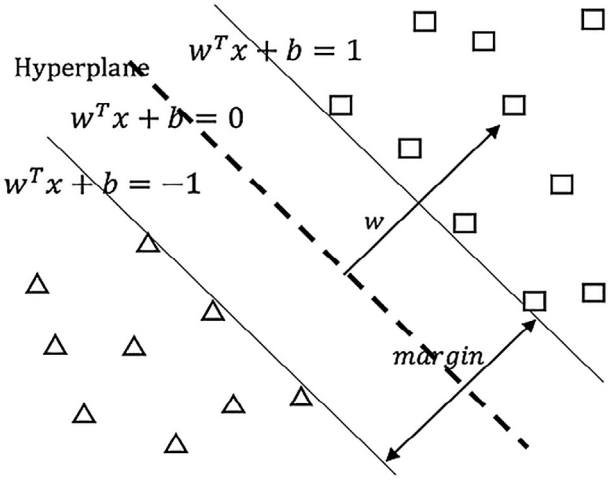

Fig. 7. Linear support vector machine.

$$Specificity = \frac{TN}{TN + FP} \times 100\% \quad (25)$$

where TP, FP, TN, FN are abbreviations for true positive, false positive, true negative and false negative, respectively [30].

3. Results and discussion

The main goal of this study was to develop an efficient algorithm for early detection of diabetic foot with infrared thermal images using asymmetry analysis of temperature and texture features. Sixty subjects participated voluntarily in the present work out of which 24 are from the control group and 36 from the DM group. The left and right foot regions are segmented using region growing algorithm from color images. The binary image of the segmented foot regions was multiplied with the red, green and blue planes of the respective foot thermal images and concatenated together to get the segmented foot regions from the thermal image. Similarly, the binary image of the segmented foot regions was multiplied with the temperature profile of the corresponding foot regions to obtain the temperature distribution for foot regions. 11 ROIs which are prone to ulcer were selected from segmented left and right foot of thermal images and temperature profiles. 12 texture features which are represented as co-occurrence features and 2 temperature features were extracted from all the ROIs for left and right foot regions.

Asymmetry analysis was used to find the difference in the extracted texture and temperature features between ipsilateral and contralateral foot regions (ROIs). All the regions (ROIs) were taken as separate input for finding the asymmetry in extracted features, which results in 11 ROIs for a single subject and 660 regions for 60 subjects. In the control group, the asymmetry in texture features was found to be small due to the symmetric nature of foot thermogram but was not so in patients with diabetic foot complications. The mean value and standard deviation of the asymmetry in the extracted temperature and texture features were computed for both the control group and the DM group, which are tabulated in Table.1. The methodology adopted in this work can be used as a baseline for further comparison and early identification of diabetic foot complications to avoid the amputation of the lower extremity. The SVM classifier is trained with asymmetry features of 140 regions (70 from the control group and 70 from the DM group) and tested with the remaining 520 regions. The performance of the SVM classifier to classify the test data into normal and prone to the ulcer is tabulated in Table.2.

Table 1
Asymmetry in extracted features.

Features	Mean ± Standard deviation	
	Control group	Diabetic group
Mean Temperature	0.48 ± 0.36	3.18 ± 0.86
SD of Temperature	0.05 ± 0.04	0.11 ± 0.17
Auto Correlation	5.10 ± 5.54	16.15 ± 11.30
Contrast	0.17 ± 0.22	0.17 ± 0.20
Correlation	0.19 ± 0.23	0.19 ± 0.21
Dissimilarity	0.11 ± 0.10	0.11 ± 0.08
Energy	0.17 ± 0.16	0.25 ± 0.20
Entropy	0.48 ± 0.37	0.66 ± 0.47
Homogeneity	0.05 ± 0.04	0.05 ± 0.04
Maximum Probability	0.18 ± 0.14	0.24 ± 0.18
Sum of Squares: Variance	5.06 ± 5.59	16.08 ± 11.20
Sum Average	1.36 ± 1.25	3.19 ± 2.45
Sum Variance	18.22 ± 21.60	61.88 ± 40.05
Sum Entropy	0.44 ± 0.36	0.61 ± 0.43

Table 2
Performance of the SVM classifier.

Performance measures	Value (in %)
Accuracy	95.61
Sensitivity	96.50
Specificity	92.41

4. Conclusion

A computer-assisted diagnostic system for the early detection of diabetic foot ulcer is developed. In this study, the texture features are extracted along with temperature features. The 11 ROIs which are prone to get ulceration in both left and right foot regions are selected from thermal images and temperature profiles. The 2 temperature features and 12 GLCM texture features were extracted and the asymmetry analysis was performed between the ipsilateral and contralateral regions of the foot. The features are classified into normal and ulcer using SVM classifier with an accuracy of 95.61%, sensitivity of 96.5% and specificity of 92.41%. The performance achieved by the proposed method was significantly better than the other methods reported in the literature. The study concludes that asymmetry analysis of texture and temperature features extracted from acquired plantar foot thermal images and temperature profiles were able to detect the diabetic foot ulceration. In future studies, the texture features extracted from color images which are essential for early identification of diabetic foot complications can be combined to extend the promising early findings obtained in the study.

Funding

This research did not receive any specific grant from funding agencies in the public, commercial, or not-for-profit sectors in the subject matter or materials discussed in this manuscript.

Acknowledgement

The authors are thankful to the patients and healthy volunteers who actively participated in the data collection and the clinicians in the Hycare for Wounds, Chennai.

Declaration of Competing Interest

The authors declare that there is no conflict of interests regarding the publication of this paper.

Appendix A. Supplementary material

Supplementary data to this article can be found online at https://doi.org/10.1016/j.infrared.2020.103219.

References

[1] American Diabetes Association, Diagnosis and classification of diabetes mellitus, Diabetes Care 37 (Supplement 1) (2014) S81–S90.
[2] Paula Sousa, Virginie Felizardo, Daniel Oliveira, Rafael Couto and Nuno M Garcia, Expert Review of Medical Devices, A review of thermal methods and technologies for diabetic foot assessment, 2015, pp. 1–10.
[3] Y. Liu, A. Polo, M. Zequera, R. Harba, R. Canals, Vilcahuaman L and Bello Y, Detection of Diabetic Foot Hyperthermia by using a regionalization method, based, on the plantar angiosomes, on Infrared Images, Proceedings 38th Annual International Conference of the IEEE Engineering in Medicine and Biology Society (EMBC), 2016, pp. 1389–1392.
[4] Makoto Oe, Rie Roselyne Yotsu, Hiromi Sanada, Takashi Nagase, Takeshi Tamaki, Screening for osteomyelitis using thermography in patients with diabetic foot, Ulcers 2013 (2013) 1–6.
[5] Luay Fraiwan, Mohanad AlKhodari, Jolu Ninan, Basil Mustafa, Adel Saleh, Mohammed Ghazal, Diabetic foot ulcer mobile detection system using smart phone thermal camera: a feasibility study, Biomed. Eng. Online 16 (117) (2016) 1–19.
[6] Chanjuan Liu, Ferdi van der Heijden, Marvin E. Klein, Jeff G. van Baal, Sicco A. Bus, Jaap J. van Netten, Infrared dermal thermography on diabetic feet soles to predict ulcerations: a case study, Adv. Biomed. Clin. Diagnostic Syst. XI, 2013, vol. 8572; pp. 87520N-1 – 9.
[7] Luciane Fachin, Balbinot Caroline, Cabral Robinson, Matilde Achaval, Milton Antônio Zaroand, Marcos Leal Brioschi, Repeatability of infrared plantar thermography in diabetes patients: a pilot study, J. Diabet. Sci. Technol. 7 (5) (2013) 1130–1137.
[8] L. Vilcahuaman, R. Harba, R. Canals, M. Zequera, C. Wilches, M.T. Arista, L. Torres, H. Arbañil, Detection of Diabetic Foot Hyperthermia by Infrared Imaging, Proceedings 36th Annual International Conference of the IEEE Engineering in Medicine and Biology Society (EMBC), 2014, pp. 4831–4834.
[9] Alfred Gatt, Cynthia Formosa, Kevin Cassar, Kenneth P. Camilleri, Clifford De Raffaele, Anabelle Mizzi, Carl Azzopardi, Stephen Mizzi, Owen Falzon, Stefania Cristina, Nachiappan Chockalingam, Thermographic patterns of the upper and lower limbs: baseline data, Int. J. Vascular Med. 2015 (2014) 1–9.
[10] D. Hernandez-Contreras, H. Peregrina-Barreto, J. Rangel-Magdaleno, J. Ramirez-Cortes, F. Renero-Carrillo, and G. Avina-Cervantes, Evaluation of thermal patterns and distribution applied to the study of diabetic foot, Proceedings IEEE International Instrumentation and Measurement Technology Conference (I2MTC), 2015; pp.1–6.
[11] E.F.J. Ring, K. Ammer, Infrared thermal imaging in medicine, Physiol. Meas. (2012) R33–R46.
[12] Ruben Usamentiaga, Pablo Venegas, Jon Guerediaga, Laura Vega, Julio Molleda, Francisco G. Bulnes, Infrared thermography for temperature measurement and non-destructive testing, Sensors 14 (2014) 12305–12348.
[13] Lawrence A. Lavery, Kevin R. Higgins, Dan R. Lanctot, George P. Constantinides, Ruben G. Zamorano, David G. Armstrong, A. Kyriacos, C. Athanasiou, Mauli Agrawal, Home monitoring of foot skin temperatures to prevent ulceration, J. Diabetes Care 27 (11) (2004) 2642–2647.
[14] Jaap J. van Netten, Jeff G. van Baal, Chanjuan Liu, Ferdi van der Heijden, Sicco A. Bus, Infrared thermal imaging for automated detection of diabetic foot complications, J. Diabetes Sci. Technol. 7 (5) (2013) 1122–1129.
[15] Constantijn E.V.B. Hazenberg, Jaap J. van Netten, G. van Sjef Baal, Sicco A. Bus, Assessment of signs of foot infection in diabetes patients using photographic foot imaging and infrared thermography, Diabetes Technol. Ther. 16 (6) (2014) 1–8.
[16] H. Peregrina-Barreto, L.A. Morales-Hernandez, J.J. Rangel-Magdaleno, J.G. Avina-Cervantes, J.M. Ramirez-Cortes, R. Morales-Caporal, Quantitative estimation of temperature variations in plantar angiosomes: a study case for diabetic foot, Comput. Math. Methods Med. 2014 (2014) 1–10.
[17] N. Pappanas, K. Papatheodorou, D. Papazoglou, C. Monastiriotis, E. Maltezoz, Foot temperature in type 2 diabetic patients with or without peripheral neuropathy, Exp. Clin. Endocrinol. Diabetes 117 (1) (2009) 44–47.
[18] Naima Kaabouch, Yi Chen, Wen-Chen Hu, Julie Anderson, Forrest Ames, and Rolf Paulson, Early Detection of Foot Ulcers through Asymmetry Analysis, Medical Imaging 2009: Biomedical Applications in Molecular, Structural, and Functional Imaging, 2009, vol.7262; pp.72621L-1 – 9.
[19] Chanjuan Liu, Jaap J. van Netten, Jeff G. van Baal, Sicco A. Bus, Ferdi van der Heijden, Automatic detection of diabetic foot complications with infrared thermography by asymmetric analysis, J. Biomed. Opt. 20 (2) (2015) pp. 026003 (1–10).
[20] F.L.I.R. Systems, Thermal Imaging Camera-Model E60, Technical data (2016).
[21] Institute for Advanced Computer Technology, Technical Report, Standards, and Protocols in Clinical Thermographic Imaging, Thermography guidelines, 2002.
[22] V. Sheeja Francis, M. Sasikala, Automatic detection of abnormal breast thermograms using asymmetry analysis of texture features, J. Med. Eng. Technol. 37 (1) (2013) 17–21.
[23] Mahnaz Etehadtavakol, Eddie Y.K. Ng, Assessment of foot complications in diabetic patients using thermography: a review, Appl. Infrared Biomed. Sci. 1 (1) (2017) 33–43.
[24] Jean Gauci, Owen Falzon, Cynthia Formosa, Alfred Gatt, Christian Ellul, Stephen Mizzi, AnabelleMizzi Cassandra, Sturgeon Delia, Kevin Cassar, Nachiappan Chockalingam, Kenneth P. Camilleri, Automated region extraction from thermal images for peripheral vascular disease monitoring, J. Healthcare Eng. 2018 (2018) 1–15.
[25] Patrick Nigri Happ, Raul Queiroz Feitosa, Cristiana Bentes, Ricardo Farias, A region-growing segmentation algorithm for GPUs, IEEE Geosci. Remote Sens. Lett. 10 (6) (2013) 1612–1616.
[26] A.J.M. Boulton, F.A. Gries, J.A. Jervell, Guidelines for the diagnosis and outpatient management of diabetic peripheral neuropathy, Diabet. Med. 15 (6) (1998) 508–514.
[27] Audrey Macdonald, Nina Petrova, Suhail Ainarkar, John Allen, Peter Plassmann, Aaron Whittam, John Bevans, Francis Ring, Ben Kluwe, Rob Simpson, Leon Rogers, Graham Machin, Mike Edmonds, Thermal symmetry of healthy feet: a precursor to a thermal study of diabetic feet prior to skin breakdown, Physiol. Measur. Inst. Phys. Eng. Med. 38 (2017) 33–44.
[28] Robert M. Haralick, K. Shanmugam, Its'hak Dinstein, Textural features for image classification, IEEE Trans. Syst. Man Cybernet. 3 (6) (1973) 610–621.
[29] Leen-Kiat Soh, Costas Tsatsoulis, Texture analysis of SAR sea ice imagery using gray level co-occurrence matrices, IEEE Trans. Geosci. Remote Sens. 37 (2) (1999) 780–795.
[30] M. Sasikala, N. Kumaravel, A wavelet-based optimal texture feature set for classification of brain tumours, J. Med. Eng. Technol. 32 (3) (2008) 198–205.
[31] P. Manika, K.M. Patit, Balasubramanian, V.B. Narayanamurthy, R. Parivalavan, Foot sole soft tissue characterization in diabetic neuropathy using texture analysis, in: Proceedings of the Biomechanics Conference, I.I.T, Delhi, Dec.2004, pp 26–33.
[32] Zhuping Zhou, Jiwei Yang, Yong Qi, Yifei Cai, Support vector machine and back propagation neutral network approaches for trip mode prediction using mobile phone data, IET Intel. Transport Syst. 12 (10) (2018) 1220–1226.
[33] Naima Kaabouch, Yi Chen, Julie Anderson, Forrest Ames, Rolf Paulson, Asymmetry analysis based on genetic algorithms for the prediction of foot ulcers, visualization and data, Analysis 7243 (2009) pp. 724304–1 – 6.
[34] Audrey Macdonald, Nina Petrova, Suhail Ainarkar, John Allen, Peter Plassmann, Aaron Whittam, John Bevans, Francis Ring, Ben Kluwe, Rob Simpson, Leon Rogers, Graham Machin, Mike Edmonds, Thermal symmetry of healthy feet: a precursor to a thermal study of diabetic feet prior to skin breakdown, Physiol. Meas. 2017 (38) (2017) 33–44.
[35] S. Madhava Prabhu, Seema Verma, A Systematic Literature Review for Early Detection of Type, II Diabetes, Proceedings IEEE International Conference on Advanced Computing & Communication Systems (ICACCS), 2019, pp. 1–5.
[36] S. Madhava Prabhu, Seema Verma, Comparative analysis of segmentation techniques for progressive evaluation and risk identification of diabetic foot ulcers, in: Proceedings IEEE 4th MEC International Conference on Big Data and Smart City (ICBDSC), 2019; pp.1–6.
[37] Daniel Alejandro Hernandez-Contreras, Hayde Peregrina-Barreto, Jose De Jesus Rangel-Magdaleno, Francisco Javier Renero-Carrillo, Plantar thermogram database for the study of diabetic foot complications, IEEE Access 7 (2019) 161296–161307.
[38] Arjaleena Ilo, Pekka Romsi, Jussi Mäkelä, Infrared thermography and vascular disorders in diabetic feet, J. Diabetes Sci. Technol. 14 (1) (2019) 28–36.